 CMES, vol.58, no.1, pp.45-73, 2010

BEM Solutions for 2D and 3D Dynamic Problems in Mindlin's Strain Gradient Theory of Elasticity[1]

A. Papacharalampopoulos[2], G. F. Karlis[2], A. Charalambopoulos[3] and D. Polyzos[4]

Abstract: A Boundary Element Method (BEM) for solving two (2D) and three dimensional (3D) dynamic problems in materials with microstructural effects is presented. The analysis is performed in the frequency domain and in the context of Mindlin's Form II gradient elastic theory. The fundamental solution of the differential equation of motion is explicitly derived for both 2D and 3D problems. The integral representation of the problem, consisting of two boundary integral equations, one for displacements and the other for its normal derivative is exploited for the proposed BEM formulation. The global boundary of the analyzed domain is discretized into quadratic line and quadrilateral elements for 2D and 3D problems, respectively. Representative 2D and 3D numerical examples are presented to illustrate the method, demonstrate its accuracy and efficiency and assess the gradient effect on the response.

Keywords: Microstructure, Microintertia, Gradient Elasticity, Mindlin, Fundamental Solution, Dispersion, BEM.

1 Introduction

When the dimensions of a structure become comparable to the size of the microstructure of the medium, size effects are observed. This means that specimens with similar shape but different dimensions appear different response to the same loading. The phenomenon is more complicated in dynamic problems where both

[1] This paper is dedicated to the memory of Professor Ioannis Vardoulakis.

[2] Department of Mechanical and Aeronautical Engineering, University of Patras, GR-26500 Patras, Greece

[3] Department of Materials Science and Engineering University of Ioannina, Dourouti, Ioannina, Greece

[4] Department of Mechanical and Aeronautical Engineering, University of Patras, GR-26500 Patras, Greece & Institute of Chemical Engineering and High Temperature Process, ICETH-FORTH, Rio, Greece

stiffness and inertia are affected by the presence of the microstructure. It is well known that due to the lack of internal length scale parameters classical theory elasticity fails to describe such a behavior. However, this is possible with the use of other enhanced elastic theories where intrinsic parameters correlating the microstructure with the macrostructure are involved in the constitutive equations as well as in the equation of motion of the considered elastic continuum. Such theories and the most general are those known in the literature as Cosserat elastic theory (Cosserat and Cosserat (1909)), Cosserat theory with constrained rotations or couple stresses theory (Mindlin and Tiersten (1962), Koiter (1964)) strain gradient theory (Toupin (1962)), multipolar elastic theory (Green(1964)), higher order strain gradient elastic theory (Mindlin (1964, 1965)), micromorphic, microstretch and micropolar elastic theories (Eringen (1999)) and non-local elasticity (Eringen (1992)). Among these theories, one can say that the most widely used are those of micropolar and gradient elasticity (Kadowaki and Liu (2005), Xie and Long (2006), Chen and Lee (2004), Teneketzis and Aifantis (2002) and Karlis, Tsinopoulos, Polyzos and Beskos (2008)).

The present work reports a boundary element formulation of Form II strain gradient elastic theory, which is a special case of Mindlin's general strain gradient elasticity (Mindlin (1964, 1965)). The static version of this formulation is presented in the very recent paper of Karlis, Charalambopoulos and Polyzos (2010). Mindlin in the middle of 60's proposed an enhanced general elastic theory to describe linear elastic behavior of isotropic materials with microstructural effects. He considered the potential energy density as a quadratic form not only of strains but also of gradient of strains. Similarly, the kinetic energy density was a quadratic form of both velocities and gradient of velocities. However, in order to balance the dimensions of strains/velocities and higher order gradients of strains/velocities, Mindlin utilized a plethora of new constants rendering thus his general theory very complicated from physical and mathematical point of view. In order to make things simpler Mindlin proposed three simplified versions of his theory, known as Form I, II and III, utilizing in the final constitutive equations only two material and five internal length scale constants instead of eighteen employed in his initial model. The basic assumptions made were motion in low frequencies and the same deformation for macro and micro structure. In Form-I, the strain energy density function is assumed to be a quadratic form of the classical strains and the second gradient of displacement; in Form-II the second gradient displacement is replaced by the gradient of strains and in Form-III the strain energy function is written in terms of the strain, the gradient of rotation, and the fully symmetric part of the gradient of strain. Although the three forms are equivalent and conclude to the same equation of motion, the Form-II leads to a total stress tensor, which is symmetric as in the

case of classical elasticity thus avoiding problems associated with non-symmetric stress tensors introduced by Cosserat and couple stress theories.

Due to the complexity of Mindlin's theory, analytical solution even for regular shaped materials is a very difficult task. Thus, resort should be made to numerical methods such as the Finite Element Method (FEM), the Boundary Element Method (BEM) or the Meshless Methods (MM). Although the FEM is the most widely used numerical method for solving elastic problems, it appears the disadvantage of requiring elements with $C^{(1)}$ continuity (Zervos (2000), Papanikolopoulos, Zervos and Vardoulakis (2009)), since the presence of higher order gradients in the expression of potential energy leads to an equilibrium equation represented by a forth order partial differential operator. To author's best knowledge, in the framework of dynamic problems there are not papers dealing with FEM solutions of Mindlin's Form II gradient elastic problems. There are however FEM solutions for simpler gradient elastic models all special cases of Mindlin's Form II gradient elastic theory. More precisely, the dipolar gradient elastic theory, illustrated in Georgiadis (2003), has been implemented through a mixed FEM formulation by Markolefas, Tsouvalas, and Tsamasphyros(2007, 2009). However, as in the static case, mixed formulations are associated with problems dealing with locking and increase of the degrees of freedom of the problem due to many interpolated fields. Askes, Bennett and Aifantis (2007), Askes, Wang and Bennett (2008) and Bennett and Askes (2009) exploiting a gradient elastic model proposed by Aifantis, also a simple special case of Mindlin's Form II theory, solved dynamic gradient elastic problems through a FEM displacement formulation. The main problem with those papers is that due to the complete lack of a variational formulation, the considered boundary conditions are not compatible with the corresponding correct ones provided by Mindlin.

On the other hand, the BEM is a well-known and powerful numerical tool, successfully used in recent years to solve various types of engineering problems (Beskos (1987, 1997)). A remarkable advantage it offers as compared to FEM is the reduction of the dimensionality of the problem by one. Thus, three dimensional problems are accurately solved by discretizing only two-dimensional surfaces surrounding the domain of interest. In the case where the problem is characterized by an axisymmetric geometry, the BEM reduces further the dimensionality of the problem, requiring just a discretization along a meridional line of the body. These advantages in conjunction with the absence of $C^{(1)}$ continuity requirements, render the BEM ideal for analyzing gradient elastic problems. Tsepoura, Papargyri-Beskou and Polyzos (2002) were the first to use BEM for solving elastostatic problems in the framework of gradient elastic theories. This work was followed by the publications Tsepoura and Polyzos (2002), Polyzos, Tsepoura, Tsinopoulos and Beskos

(2003), Tsepoura, Polyzos, Tsinopoulos and Beskos (2003), Polyzos, Tsepoura, Tsinopoulos and Beskos (2005), Polyzos (2005), Karlis, Tsinopoulos, Polyzos and Beskos (2007, 2008), which are the only papers dealing with two and three dimensional BEM solutions of static and dynamic gradient elastic and fracture mechanics problems. All these papers implement two simple gradient elastic models, with the first being the simplest possible special case of Mindlin's Form II strain gradient elastic theory and the second an enrichment of the simple gradient elastic model with surface energy terms which affect only the boundary conditions of the problem (Vardoulakis and Sulem (1995), Exadaktylos and Vardoulakis (2001)). Although micropolar elastic theory is different to that of gradient elasticity, it should be mentioned here the works of Sladek and Sladek (1985 I, II, III), Liang and Huang (1996) and Huang and Liang (1997) as BEM formulations for enhanced theories.

Recently, Atluri and co-workers proposed the Local Boundary Integral Equation (LBIE) method (Zhu, Zhang, and Atluri (1998)) and the Meshless Local Petrov-Galerkin (MLPG) method (Atluri and Zhu (1998)) as alternatives to the BEM and FEM, respectively. Both methods are characterized as "truly meshless" since no background cells are required for the numerical evaluation of the involved integrals. Properly distributed nodal points, without any connectivity requirement, covering the domain of interest as well as the surrounding global boundary are employed instead of any boundary or finite element discretization. All nodal points belong in regular sub-domains (e.g. circles for two-dimensional problems) centered at the corresponding collocation points. The fields at the local and global boundaries as well as in the interior of the subdomains are usually approximated by the Moving Least Squares (MLS) approximation scheme. Owing to regular shapes of the sub-domains, both surface and volume integrals are easily evaluated. The local nature of the sub-domains leads to a final linear system of equations the coefficient matrix of which is sparse and not fully populated. Both methods are ideal for treating gradient elastic problems since they utilize MLS interpolation functions, which are $C^{(1)}$ by definition. Recently, Tang, Shen and Atluri (2003) employing the MLPG method solved 2D gradient elastostatic problems in the framework of Mindlin's general gradient elastic theory, while Sladek and Sladek (2003) proposed a LBIE method for solving micropolar elastic problems. More details for MLPG and LBIE methods one can find in Sladek, Sladek and Solek (2009), Atluri and Shen (2002), Han and Atluri (2004) and Atluri (2004).

In the present paper the BEM in its direct form is employed for the solution of two-dimensional (2D) and three-dimensional (3D) dynamic problems in the framework of the Form-II strain-gradient theory of Mindlin. The paper consists of the following six sections: Section 2 presents the Form II version of Mindlin's general strain gradient elastic theory. In Section 3, the 2D and 3D fundamental solutions of the

problem are explicitly derived. Section 4 demonstrates the integral representation of the gradient elastic boundary value problem as well as details of the proposed BEM formulation, while Section 5 provides three numerical examples (2D and 3D) to demonstrate the accuracy of the method and illustrate the microstructural effects. Finally, Section 6 consists of the conclusions pertaining to this work.

2 The Form-II dynamic strain gradient elastic theory of Mindlin

In this section the higher order gradient elastic theory of Mindlin exploited in the present work is explained.

Mindlin (1964) in the Form II version of his general strain gradient elastic theory considered that the potential energy W of an isotropic elastic body with microstructure of volume V is a quadratic form of the strains ε_{ij} and the gradient of strains, κ_{ijk} i.e.,

$$W = \int_V (\frac{1}{2}\tilde{\lambda}\varepsilon_{ii}\varepsilon_{jj} + \tilde{\mu}\varepsilon_{ij}\varepsilon_{ij} + \hat{\alpha}_1\kappa_{iik}\kappa_{kjj} + \hat{\alpha}_2\kappa_{ijj}\kappa_{ikk} + \hat{\alpha}_3\kappa_{iik}\kappa_{jjk} + \hat{\alpha}_4\kappa_{ijk}\kappa_{ijk} + \hat{\alpha}_5\kappa_{ijk}\kappa_{kji})dV \quad (1)$$

where

$$\varepsilon_{ij} = \frac{1}{2}(\partial_i u_j + \partial_j u_i) \quad (2)$$

$$\kappa_{ijk} = \partial_i\varepsilon_{jk} = \frac{1}{2}(\partial_i\partial_j u_k + \partial_i\partial_k u_j) = \kappa_{ikj} \quad (3)$$

$$\tilde{\mu} = \mu - \frac{2g_2^2}{b_2+b_3}, \quad \tilde{\lambda} + 2\tilde{\mu} = \lambda + 2\mu - \frac{8g_2^2}{3(b_2+b_3)} - \frac{(3g_1+2g_2)^2}{3(3b_1+b_2+b_3)} \quad (4)$$

with ∂_i denoting space differentiation, u_i displacements, λ, μ the Lamé constants and $\hat{\alpha}_1 \div \hat{\alpha}_5$, $g_1, g_2, b_1 \div b_3$ intrinsic constants coming from the presence of microstructure, all explicitly defined in Mindlin (1964).

Strains ε_{ij} and gradient of strains κ_{ijk} are dual in energy with the Cauchy-like and double stresses, respectively, defined as

$$\tau_{ij} = \frac{\partial W}{\partial \varepsilon_{ij}} = \tau_{ji} \quad (5)$$

$$\mu_{ijk} = \frac{\partial W}{\partial \kappa_{ijk}} = \mu_{ikj} \quad (6)$$

which implies that

$$\tau_{ij} = 2\tilde{\mu}\varepsilon_{ij} + \tilde{\lambda}\varepsilon_{ll}\delta_{ij} \tag{7}$$

and

$$\begin{aligned}\mu_{ijk} =& \frac{1}{2}\hat{\alpha}_1\left[\kappa_{kll}\delta_{ij} + 2\kappa_{lli}\delta_{jk} + \kappa_{jll}\delta_{ki}\right] + 2\hat{\alpha}_2\kappa_{ill}\delta_{jk} + \\ &+ \hat{\alpha}_3(\kappa_{llk}\delta_{ij} + \kappa_{llj}\delta_{ik}) + 2\hat{\alpha}_4\kappa_{ijk} + \hat{\alpha}_5\left(\kappa_{kij} + \kappa_{jki}\right)\end{aligned} \tag{8}$$

Extending the idea of non locality to the inertia of the continuum with microstructure, Mindlin proposed a new expression for the kinetic energy density function where the gradients of the velocities are taken into account, i.e.

$$T = \int_V (\frac{1}{2}\rho\dot{u}_i\dot{u}_i + \frac{1}{6}\rho' d^2_{pkmn}\partial_m\dot{u}_n\partial_p\dot{u}_k)dV \tag{9}$$

$$\begin{aligned}d^2_{pkmn} &= d^2_{mnpk} \\ &= \frac{1}{2}d^2\left[\delta_{pm}\delta_{kn} - \delta_{pn}\delta_{km} + 2\alpha(3\alpha+2\beta)\delta_{pk}\delta_{mn} + \beta^2(\delta_{pm}\delta_{kn} + \delta_{pn}\delta_{km})\right]\end{aligned} \tag{10}$$

$$\alpha = \frac{1}{b_2+b_3}\left(g_1 - \frac{b_1(3g_1+2g_2)}{3b_1+b_2+b_3}\right),\ \beta = 1 + \frac{2g_2}{b_2+b_3} \tag{11}$$

where dots denote differentiation with respect to time, ρ' is the density of the microstructure, δ_{ij} stands for Kronecker delta and d is the characteristic dimension of the representative cell of the microstructure.

The dynamic governing equation of the considered gradient elastic body as well as the possible boundary conditions that establish a well-posed boundary value problem can be determined with the aid of the Hamilton's variational principle, written as

$$\int_{t_0}^{t_1}\delta(W-T)dt - \int_{t_0}^{t_1}\delta W_1 dt = 0 \tag{12}$$

where δ denotes variation and W_1 represents the work done by external forces.

Inserting Eqs. (1) and (9) into Eq. (12) and taken into account body forces F_k one obtains the following equation of motion:

$$\partial_j(\tau_{jk} - \partial_i\mu_{ijk}) + F_k = \rho\ddot{u}_k - \frac{1}{3}\partial_p(\rho' d^2_{pkmn}\partial_m\ddot{u}_n) \tag{13}$$

accompanied by the classical essential and natural boundary conditions where the displacement vector $\mathbf{u}$ and/or the traction vector $\mathbf{p}$ have to be defined on the global boundary S of the analyzed domain, the non-classical essential and natural boundary conditions where the normal displacement vector $\mathbf{q} = \partial\mathbf{u}/\partial n$ and/or the double traction vector $\mathbf{R}$ are prescribed on S and the non-classical boundary condition satisfied only when non-smooth boundaries are dealt with, where the jump traction vector $\mathbf{E}$ has to be defined at corners and edges. Traction vectors $\mathbf{p}$, $\mathbf{R}$, $\mathbf{E}$ are defined as

$$p_k = n_j\tau_{jk} - n_i n_j D\mu_{ijk} - (n_j D_i + n_i D_j)\mu_{ijk} + (n_i n_j D_l n_l - D_j n_i)\mu_{ijk} + \\ + \frac{1}{3}\rho' n_p d^2_{pkmn}(D_m\ddot{u}_n + n_m D\ddot{u}_n) \tag{14}$$

$$R_k = n_i n_j \mu_{ijk} \tag{15}$$

$$E_k = \left\| n_i m_j \mu_{ijk} \right\| \tag{16}$$

where n_i is the unit vector normal to the global boundary S, $D = n_l\partial_l$ and $D_j = (\delta_{jl} - n_j n_l)\partial_l$ is the surface gradient operator. The non-classical boundary condition (16) exists only when non-smooth boundaries are considered. Double brackets $\|\bullet\|$ indicate that the enclosed quantity is the difference between its values taken on the two sides of a corner while m_i is a vector being tangential to the corner line.

Finally, taking into account relations (7) and (8), the equation of motion (13) in terms of displacement vector is written as

$$(\tilde{\lambda} + 2\tilde{\mu})(1 - \ell_1^2\nabla^2)\nabla\nabla\cdot\mathbf{u} + \tilde{\mu}(1 - \ell_2^2\nabla^2)\nabla\times\nabla\times\mathbf{u} + \mathbf{F} \\ = \rho\left(\ddot{\mathbf{u}} - h_1^2\nabla\nabla\cdot\ddot{\mathbf{u}} + h_2^2\nabla\times\nabla\times\ddot{\mathbf{u}}\right) \tag{17}$$

or in frequency domain for the frequency ω

$$(\tilde{\lambda} + 2\tilde{\mu})(1 - \ell_1^2\nabla^2)\nabla\nabla\cdot\mathbf{u} + \tilde{\mu}(1 - \ell_2^2\nabla^2)\nabla\times\nabla\times\mathbf{u} + \mathbf{F} \\ + \rho\omega^2\left(\mathbf{u} - h_1^2\nabla\nabla\cdot\mathbf{u} + h_2^2\nabla\times\nabla\times\mathbf{u}\right) = \mathbf{0} \tag{18}$$

where

$$\ell_1^2 = 2(\hat{a}_1 + \hat{a}_2 + \hat{a}_3 + \hat{a}_4 + \hat{a}_5)/(\tilde{\lambda} + 2\tilde{\mu}) \tag{19}$$

$$\ell_2^2 = (\hat{a}_3 + 2\hat{a}_4 + \hat{a}_5)/2\tilde{\mu} \tag{20}$$

and

$$h_1^2 = \frac{\rho' d^2\left[2\alpha^2 + (\alpha+\beta)^2\right]}{3\rho} \tag{21}$$

$$h_2^2 = \frac{\rho' d^2 \left(1+\beta^2\right)}{6\rho} \tag{22}$$

The intrinsic parameters ℓ_1^2, ℓ_2^2, h_1^2, h_2^2 appearing in (17) and (18) have units of length square (m^2) and represent the effect of the stiffness (ℓ_1^2, ℓ_2^2) and the inertia (h_1^2, h_2^2) of the microstructure on the macrostructural behavior of the gradient elastic material. ℓ_1^2, h_1^2 are related to longitudinal deformations while ℓ_2^2, h_2^2 to shear ones. Positive definiteness of the potential energy requires $\tilde{\mu}$, $\tilde{\lambda}+2\tilde{\mu} > 0$, $\ell_i^2 > 0$ while $h_i^2 > 0$ by inspection.

It should be mentioned here that considering the same density throughout the analyzed domain ($\rho' = \rho$) and $\hat{\alpha}_1 = \hat{\alpha}_3 = \hat{\alpha}_5 = 0$, $\hat{\alpha}_2 = \frac{\tilde{\lambda}}{2} g^2$, $\quad \hat{\alpha}_4 = \tilde{\mu} g^2$, $g_1^2 = g_2^2 = 0$, relations (4), (10), (11), (19), (20), (21) and (22) imply that $\tilde{\lambda} \equiv \lambda$, $\tilde{\mu} \equiv \mu$, $\alpha = 0$, $\beta = 1$, $\tilde{d}^2_{pkmn} = h^2 \delta_{pm} \delta_{kn}$, $\ell_1^2 = \ell_2^2 = g^2$, $h_1^2 = h_2^2 = h^2$
which correspond to the simplest possible special case of Mindlin's general theory known as dipolar gradient elastic theory presented in Georgiadis (2003) and implemented for the BEM in Polyzos (2005).

3 2D and 3D fundamental solutions

Adopting the methodology presented in Polyzos, Tsepoura, Tsinopoulos and Polyzos (2003), the 2D and 3D fundamental solutions of the differential equation of motion (18) are explicitly derived in the present section.

For an infinitely extended gradient elastic space, the fundamental solutions are represented by a second order tensor $\tilde{\mathbf{u}}^*(\mathbf{x},\mathbf{y})$ satisfying the partial differential equation

$$\begin{aligned}&(\lambda+2\mu)\left(1-\ell_1^2\Delta_x\right)\nabla_x\nabla_x\cdot\tilde{\mathbf{u}}^*(\mathbf{x},\mathbf{y}) - \mu\left(1-\ell_2^2\Delta_x\right)\nabla_x\times\nabla_x\times\tilde{\mathbf{u}}^*(\mathbf{x},\mathbf{y}) + \delta(\mathbf{x},\mathbf{y})\tilde{\mathbf{I}} = \\ &-\rho\omega^2\left(\tilde{\mathbf{u}}^*(\mathbf{x},\mathbf{y}) - h_1^2\nabla\nabla\cdot\tilde{\mathbf{u}}^*(\mathbf{x},\mathbf{y}) + h_2^2\nabla\times\nabla\times\tilde{\mathbf{u}}^*(\mathbf{x},\mathbf{y})\right)\end{aligned} \tag{23}$$

where δ is the Dirac δ-function, $\boldsymbol{x}$ is the point where the displacement field $\tilde{\mathbf{u}}^*(\mathbf{x},\mathbf{y})$ is obtained due to a unit force at point $\boldsymbol{y}$ and $r = |\mathbf{x}-\mathbf{y}|$.

The field $\mathbf{u}^*$ can be decomposed into irrotational and solenoidal parts according to

$$\tilde{\mathbf{u}}^* = \nabla\nabla\phi + \nabla\nabla\times\mathbf{A} + \nabla\times\nabla\times\tilde{\mathbf{G}} \tag{24}$$

where $\phi(r)$ is a scalar function, $\mathbf{A}(r)$ a vector function and $\tilde{\mathbf{G}}(r)$ a tensorial function. As it is explained in Polyzos, Tsepoura, Tsinopoulos and Polyzos (2003), due to the radial nature of the fundamental solution, it is apparent that the vector $\mathbf{A}(r)$ should be equal to zero. On the other hand the Dirac δ-function can be written as

$$-\delta(r) = \nabla^2 g(r) = \nabla\nabla g(r) - \nabla\times\nabla\times\left[g(r)\tilde{\mathbf{I}}\right] \tag{25}$$

with $g(r)$ being the fundamental solution of the Laplace operator, having the form

$$g(r)=\begin{cases}\frac{1}{2\pi}\ln\frac{1}{r}\ for\ 2D\\ \frac{1}{4\pi r}\quad for\ 3D\end{cases} \tag{26}$$

Inserting (24) and (25) into (23) one obtains

$$\begin{aligned}&\nabla\nabla\left\{\left[(\lambda+2\mu)\left(1-\ell_1^2\nabla^2\right)-\rho\omega^2h_1^2\right]\nabla^2\phi(r)+\rho\omega^2\phi(r)\right\}+\\&+\nabla\times\nabla\times\left\{\left[\mu\left(1-\ell_2^2\nabla^2\right)-\rho\omega^2h_2^2\right]\nabla^2\tilde{\mathbf{G}}(r)+\rho\omega^2\tilde{\mathbf{G}}(r)\right\}=\\=&\frac{1}{2\pi}\nabla\nabla g(r)-\frac{1}{2\pi}\nabla\times\nabla\times\left(g(r)\tilde{\mathbf{I}}\right)\end{aligned} \tag{27}$$

The irrotational and solenoidal nature of $\phi(r)$ and $\tilde{\mathbf{G}}(r)$, respectively, impose that (27) is satisfied if

$$\begin{aligned}&\nabla^2\phi(r)-\ell_1^2\frac{\lambda+2\mu}{\lambda+2\mu-\rho\omega^2h_1^2}\nabla^4\phi(r)+\\&+\frac{\rho\omega^2}{\lambda+2\mu-\rho\omega^2h_1^2}\phi(r)=\frac{1}{\lambda+2\mu-\rho\omega^2h_1^2}g(r)\end{aligned} \tag{28}$$

$$\nabla^2\tilde{\mathbf{G}}(r)-\ell_1^2\frac{\mu}{\mu-\rho\omega^2h_2^2}\nabla^4\tilde{\mathbf{G}}(r)+\frac{\rho\omega^2}{\mu-\rho\omega^2h_2^2}\tilde{\mathbf{G}}(r)=\frac{1}{\mu-\rho\omega^2h_2^2}g(r)\tilde{\mathbf{I}} \tag{29}$$

For $\omega^2\neq(\lambda+2\mu)/(\rho h_1^2)$ and $\omega^2\neq\mu/(\rho h_2^2)$ it is not difficult to find one that the solutions of the above two partial differential equations are, respectively

$$\phi(r)=\frac{1}{2\pi\rho\omega^2}\left\{-\ln r-\frac{1+L_1^2k_1^2}{1+2L_1^2k_1^2}K_0(ik_1r)-\frac{L_1^2k_1^2}{1+2L_1^2k_1^2}K_0(\alpha_1r)\right\} \tag{30}$$

$$\tilde{\mathbf{G}}(r)=-\frac{1}{2\pi\rho\omega^2}\left\{-\ln r-\frac{1+L_2^2k_2^2}{1+2L_2^2k_2^2}K_0(ik_2r)-\frac{L_2^2k_2^2}{1+2L_2^2k_2^2}K_0(\alpha_2r)\right\}\tilde{\mathbf{I}} \tag{31}$$

for two dimensions and

$$\phi(r)=\frac{1}{4\pi\rho\omega^2}\left(\frac{1}{r}-\frac{1+L_1^2k_1^2}{1+2L_1^2k_1^2}\frac{e^{-ik_1r}}{r}-\frac{L_1^2k_1^2}{1+2L_1^2k_1^2}\frac{e^{-\alpha_1r}}{r}\right) \tag{32}$$

$$\tilde{\mathbf{G}}(r)=\frac{1}{4\pi\rho\omega^2}\left\{\frac{1}{r}-\frac{1+L_2^2k_2^2}{1+2L_2^2k_2^2}\frac{e^{-ik_2r}}{r}-\frac{L_2^2k_2^2}{1+2L_2^2k_2^2}\frac{e^{-\alpha_2r}}{r}\right\}\tilde{\mathbf{I}} \tag{33}$$

for three dimensions.

$K_n(\bullet)$ represents the modified Bessel functions of second kind and nth order, k_1^2, k_2^2 satisfy the dispersions relations $k_1^2\left(1+L_1^2k_1^2\right)=k_P^2$ and $k_2^2\left(1+L_2^2k_2^2\right)=k_S^2$, respectively, while

$$k_P=\sqrt{\frac{\rho\omega^2}{\lambda+2\mu-\rho\omega^2h_1^2}},\quad k_S=\sqrt{\frac{\rho\omega^2}{\mu-\rho\omega^2h_2^2}} \tag{34}$$

$$L_1=\ell_1\sqrt{\frac{\lambda+2\mu}{\lambda+2\mu-\rho\omega^2h_1^2}},\ L_2=\ell_2\sqrt{\frac{\mu}{\mu-\rho\omega^2h_2^2}} \tag{35}$$

and

$$\alpha_1=\sqrt{\frac{1}{L_1^2}+k_1^2},\ \alpha_2=\sqrt{\frac{1}{L_2^2}+k_2^2} \tag{36}$$

Inserting (30)-(33) in (24), the fundamental solution $\tilde{\mathbf{u}}^*(\mathbf{x},\mathbf{y})$ obtains the final form

$$\tilde{u}_{ij}^*=\frac{1}{2^{\alpha-1}\pi\rho\omega^2}\left[\Psi(r)\,\delta_{ij}-\mathrm{X}(r)\,\hat{r}_i\hat{r}_j\right] \tag{37}$$

Where α is the dimensionality of the problem (2 for 2D and 3 for 3D), $\hat{\mathbf{r}}=\frac{\mathbf{x}-\mathbf{y}}{|\mathbf{x}-\mathbf{y}|}$ and

$$\begin{aligned}\mathrm{X}(r)=&-\left[\frac{1+L_1^2k_1^2}{1+2L_1^2k_1^2}k_1^2K_2(ik_1r)-\frac{1+L_2^2k_2^2}{1+2L_2^2k_2^2}k_2^2K_2(ik_2r)\right.\\&\left.-\frac{1+L_1^2k_1^2}{1+2L_1^2k_1^2}k_1^2K_2(a_1r)+\frac{1+L_2^2k_2^2}{1+2L_2^2k_2^2}k_2^2K_2(a_1r)\right]\end{aligned} \tag{38}$$

$$\begin{aligned}\Psi(r)=&-\frac{1+L_1^2k_1^2}{1+2L_1^2k_1^2}\frac{k_1^2}{2}\left[K_2(ik_1r)-K_0(ik_1r)\right]+\frac{1+L_2^2k_2^2}{1+2L_2^2k_2^2}\frac{k_2^2}{2}\left[K_2(ik_2r)+K_0(ik_2r)\right]\\&-\frac{1+L_1^2k_1^2}{1+2L_1^2k_1^2}\frac{k_1^2}{2}\left[K_0(a_1r)-K_2(a_1r)\right]-\frac{1+L_2^2k_2^2}{1+2L_2^2k_2^2}\frac{k_2^2}{2}\left[K_0(a_2r)+K_2(a_2r)\right]\end{aligned} \tag{39}$$

for two dimensions and

$$\begin{aligned}\mathrm{X}(r)=&-\left[\frac{1+L_1^2k_1^2}{1+2L_1^2k_1^2}\left(k_1^2-\frac{3ik_1}{r}-\frac{3}{r^2}\right)\frac{e^{-ik_1r}}{r}-\frac{1+L_2^2k_2^2}{1+2L_2^2k_2^2}\left(k_2^2-\frac{3ik_2}{r}-\frac{3}{r^2}\right)\frac{e^{-ik_2r}}{r}\right.\\&\left.-\frac{L_1^2k_1^2}{1+2L_1^2k_1^2}\left(a_1^2+\frac{3a_1}{r}+\frac{3}{r^2}\right)\frac{e^{-a_1r}}{r}+\frac{L_2^2k_2^2}{1+2L_2^2k_2^2}\left(a_2^2+\frac{3a_2}{r}+\frac{3}{r^2}\right)\frac{e^{-a_2r}}{r}\right]\end{aligned}$$

(40)

$$\Psi(r) = \frac{1+L_1^2k_1^2}{1+2L_1^2k_1^2}\left(\frac{ik_1}{r}+\frac{1}{r^2}\right)\frac{e^{-ik_1r}}{r} - \frac{1+L_2^2k_2^2}{1+2L_2^2k_2^2}\left(-k_2^2+\frac{ik_2}{r}+\frac{1}{r^2}\right)\frac{e^{-ik_2r}}{r} + \frac{L_1^2k_1^2}{1+2L_1^2k_1^2}\left(\frac{a_1}{r}+\frac{1}{r^2}\right)\frac{e^{-a_1r}}{r} - \frac{L_2^2k_2^2}{1+2L_2^2k_2^2}\left(a_2^2+\frac{a_2}{r}+\frac{1}{r^2}\right)\frac{e^{-a_2r}}{r} \tag{41}$$

for three dimensions.

The cases where $\omega^2 = (\lambda+2\mu)/(\rho h_1^2)$ and $\omega^2 = \mu/(\rho h_2^2)$, are both beyond interest since they correspond to wavelength being of the size of the microstructure.

4 Integral representation of the problem and BEM formulation

Consider a gradient elastic body of volume V, surrounded by a surface S, subjected to an external harmonic loading and satisfying the equation of motion (18) as well as certain classical and non-classical boundary conditions explained in section 2.

Symbolizing by $\mathbf{u},\mathbf{p},\mathbf{R},\mathbf{E},\mathbf{F}$ and $\mathbf{u}^*,\mathbf{p}^*,\mathbf{R}^*,\mathbf{E}^*,\mathbf{F}^*$ two deformation states of the same body, it has been proved [Tsepoura, Papargyri-Beskou and Polyzos (2002), Giannakopoulos, Amanatidou and Aravas (2006)] that the following reciprocal identity is valid

$$\int_V \{\mathbf{F}^*\cdot\mathbf{u}-\mathbf{F}\cdot\mathbf{u}^*\}\,\mathrm{d}V + \int_S \{\mathbf{p}^*\cdot\mathbf{u}-\mathbf{p}\cdot\mathbf{u}^*\}\,\mathrm{d}S = \int_S \left\{\mathbf{R}\cdot\frac{\partial\mathbf{u}^*}{\partial n}-\mathbf{R}^*\cdot\frac{\partial\mathbf{u}}{\partial n}\right\}\mathrm{d}S \tag{42}$$

for a smooth boundary S and

$$\int_V \{\mathbf{F}^*\cdot\mathbf{u}-\mathbf{F}\cdot\mathbf{u}^*\}\,\mathrm{d}V + \int_S \{\mathbf{p}^*\cdot\mathbf{u}-\mathbf{p}\cdot\mathbf{u}^*\}\,\mathrm{d}S = \int_S \left\{\mathbf{R}\cdot\frac{\partial\mathbf{u}^*}{\partial n}-\mathbf{R}^*\cdot\frac{\partial\mathbf{u}}{\partial n}\right\}\mathrm{d}S + \sum_{C_a}\oint_{C_a}\{\mathbf{E}\cdot\mathbf{u}^*-\mathbf{E}^*\cdot\mathbf{u}\}\,\mathrm{d}C \tag{43}$$

for a non-smooth boundary S,

where vectors $\mathbf{F},\mathbf{F}^*$ represent body forces and $\mathbf{p},\mathbf{R},\mathbf{E}$stand for traction, double traction and jump traction vectors, respectively, defined in (14)-(16). C_a represents the edge lines formed by the intersection of two surface portions when the boundary S is non-smooth. For a two dimensional non-smooth boundary where parts of the global boundary form C_a corners, it is easy to prove one that the reciprocal identity

(43) obtains the form

$$\int_V \{\mathbf{F}^* \cdot \mathbf{u} - \mathbf{F} \cdot \mathbf{u}^*\}\, \mathrm{d}V + \int_S \{\mathbf{p}^* \cdot \mathbf{u} - \mathbf{p} \cdot \mathbf{u}^*\}\, \mathrm{d}S = \\ = \int_S \left\{\mathbf{R} \cdot \frac{\partial \mathbf{u}^*}{\partial n} - \mathbf{R}^* \cdot \frac{\partial \mathbf{u}}{\partial n}\right\} \mathrm{d}S + \sum_{C_a} \{\mathbf{E} \cdot \mathbf{u}^* - \mathbf{E}^* \cdot \mathbf{u}\} \tag{44}$$

where

$E_k = \left\| n_i t_j \mu_{ijk} \right\|$ or $\mathbf{E} = \left\| (\hat{\mathbf{t}} \otimes \hat{\mathbf{n}}) : \mu \right\|$ (45)

with $\hat{\mathbf{t}}$ being the tantential vector to the curves forming the corner.

Assume that the displacement field $\mathbf{u}^*$, appearing in the reciprocal identity (43), is the result of a body force having the form

$$\mathbf{F}^*(\mathbf{y}) = \delta(\mathbf{x} - \mathbf{y})\, \hat{\mathbf{e}}$$

with δ being the Dirac δ-function and $\hat{\mathbf{e}}$ the direction of a unit force acting at point $\mathbf{y}$.

Recalling the definition of the fundamental solution derived in section 3, it is easy to see that the displacement field $\mathbf{u}^*$ due to $\mathbf{F}^*$ can be represented by means of the fundamental displacement tensor $\tilde{\mathbf{u}}^*(\mathbf{x}, \mathbf{y})$, given by the equation (37), according to the relation

$$\mathbf{u}^*(\mathbf{y}) = \tilde{\mathbf{u}}^*(\mathbf{x}, \mathbf{y}) \cdot \hat{\mathbf{e}} \tag{45}$$

Inserting the above expression of $\mathbf{u}^*$ in (46) and assuming zero body forces **F=0**, one obtains

$$\int_V \{\delta(\mathbf{x} - \mathbf{y})\hat{\mathbf{e}} \cdot \mathbf{u}(\mathbf{y})\}\, \mathrm{d}V_y + \int_S \{[\tilde{\mathbf{p}}^*(\mathbf{x}, \mathbf{y}) \cdot \hat{\mathbf{e}}] \cdot \mathbf{u}(\mathbf{y}) - \mathbf{p}(\mathbf{y}) \cdot [\tilde{\mathbf{u}}^*(\mathbf{x}, \mathbf{y}) \cdot \hat{\mathbf{e}}]\}\, \mathrm{d}S_y = \\ \int_S \left\{\mathbf{R}(\mathbf{y}) \cdot [\frac{\partial \tilde{\mathbf{u}}^*(\mathbf{x}, \mathbf{y})}{\partial n_y} \cdot \hat{\mathbf{e}}] - [\tilde{\mathbf{R}}^*(\mathbf{x}, \mathbf{y}) \cdot \hat{\mathbf{e}}] \cdot \frac{\partial \mathbf{u}(\mathbf{y})}{\partial n_y}\right\} \mathrm{d}S_y + \\ \sum_{C_a} \oint_{C_a} \left\{\mathbf{E}(\mathbf{y}) \cdot [\tilde{\mathbf{u}}^*(\mathbf{x}, \mathbf{y}) \cdot \hat{\mathbf{e}}] - [\tilde{\mathbf{E}}^*(\mathbf{x}, \mathbf{y}) \cdot \hat{\mathbf{e}}] \cdot \mathbf{u}(\mathbf{y})\right\} \mathrm{d}C_y \tag{46}$$

or

$$
\begin{aligned}
&(\int_V \{\delta(\mathbf{x}-\mathbf{y})\mathbf{u}(\mathbf{y})\}\, dV_y)\cdot\hat{\mathbf{e}} + (\int_S \left\{ [\tilde{\mathbf{p}}^*(\mathbf{x},\mathbf{y})]^T\cdot\mathbf{u}(\mathbf{y}) - \mathbf{p}(\mathbf{y})\cdot\tilde{\mathbf{u}}^*(\mathbf{x},\mathbf{y}) \right\} \mathrm{d}S_y)\cdot\hat{\mathbf{e}} = \\
&(\int_S \left\{ \left(\frac{\partial\tilde{\mathbf{u}}^*(\mathbf{x},\mathbf{y})}{\partial n_y} \right)^T \cdot \mathbf{R}(\mathbf{y}) - [\tilde{\mathbf{R}}^*(\mathbf{x},\mathbf{y})]^T \cdot \frac{\partial\mathbf{u}(\mathbf{y})}{\partial n_y} \right\} \mathrm{d}S_y)\cdot\hat{\mathbf{e}} + \\
&(\sum_{C_a} \oint_{C_a} \left\{ \mathbf{E}(\mathbf{y})\cdot\mathbf{u}^*(\mathbf{x},\mathbf{y}) - [\tilde{\mathbf{E}}^*(\mathbf{x},\mathbf{y})]^T\cdot\mathbf{u}(\mathbf{y}) \right\} \mathrm{d}C_y)\cdot\hat{\mathbf{e}}
\end{aligned}
\tag{47}
$$

with $\tilde{\mathbf{A}}^T$ indicating transpose of $\tilde{\mathbf{A}}$.

Considering that relation (48) is valid for any direction $\hat{\mathbf{e}}$ and taking into account the symmetry of the fundamental displacement$\tilde{\mathbf{u}}^*$, one obtains the boundary integral equation

$$
\begin{aligned}
&\tilde{\mathbf{c}}(\mathbf{x})\cdot\mathbf{u}(\mathbf{x}) + \int_S \left\{ [\tilde{\mathbf{p}}^*(\mathbf{x},\mathbf{y})]^T\cdot\mathbf{u}(\mathbf{y}) - \tilde{\mathbf{u}}^*(\mathbf{x},\mathbf{y})\cdot\mathbf{p}(\mathbf{y}) \right\} \mathrm{d}S_y = \\
&\int_S \left\{ \left(\frac{\partial\tilde{\mathbf{u}}^*(\mathbf{x},\mathbf{y})}{\partial n_y} \right)^T \cdot \mathbf{R}(\mathbf{y}) - [\tilde{\mathbf{R}}^*(\mathbf{x},\mathbf{y})]^T \cdot \frac{\partial\mathbf{u}(\mathbf{y})}{\partial n_y} \right\} \mathrm{d}S_y + \\
&\sum_{C_a} \oint_{C_a} \left\{ \mathbf{u}^*(\mathbf{x},\mathbf{y})\cdot\mathbf{E}(\mathbf{y}) - [\tilde{\mathbf{E}}^*(\mathbf{x},\mathbf{y})]^T\cdot\mathbf{u}(\mathbf{y}) \right\} \mathrm{d}C_y
\end{aligned}
\tag{48}
$$

where $\tilde{\mathbf{c}}(\mathbf{x})$ is the well known jump-tensor of classical boundary integral representations [Tsepoura, Papargyri-Beskou and Polyzos D (2002)].

Utilizing the symbols $\bar{\mathbf{U}}^*$, $\bar{\mathbf{P}}^*$, $\bar{\mathbf{Q}}^*$, $\bar{\mathbf{R}}^*$ and $\bar{\mathbf{E}}^*$ instead of $\tilde{\mathbf{u}}^*$, $(\tilde{\mathbf{p}}^*)^T$, $\left(\frac{\partial\tilde{\mathbf{u}}^*}{\partial n}\right)^T$, $\left(\tilde{\mathbf{R}}^*\right)^T$ and $\left(\tilde{\mathbf{E}}^*\right)^T$, respectively, as well as $\mathbf{q}$ instead of $\frac{\partial\mathbf{u}}{\partial n}$ Eq. (49) receives the form

$$
\begin{aligned}
&\tilde{\mathbf{c}}(\mathbf{x})\cdot\mathbf{u}(\mathbf{x}) + \int_S \left\{ \bar{\mathbf{P}}^*(\mathbf{x},\mathbf{y})\cdot\mathbf{u}(\mathbf{y}) - \bar{\mathbf{U}}^*(\mathbf{x},\mathbf{y})\cdot\mathbf{p}(\mathbf{y}) \right\} \mathrm{d}S_y = \\
&\int_S \left\{ \bar{\mathbf{Q}}^*(\mathbf{x},\mathbf{y})\cdot\mathbf{R}(\mathbf{y}) - \bar{\mathbf{R}}^*(\mathbf{x},\mathbf{y})\cdot\mathbf{q}(\mathbf{y}) \right\} \mathrm{d}S_y + \\
&\sum_{C_a} \oint_{C} \left\{ \bar{\mathbf{U}}^*(\mathbf{x},\mathbf{y})\cdot\mathbf{E}(\mathbf{y}) - \bar{\mathbf{E}}^*(\mathbf{x},\mathbf{y})\cdot\mathbf{u}(\mathbf{y}) \right\} \mathrm{d}C_y
\end{aligned}
\tag{49}
$$

Recalling (44) and (45), the above integral equation in two dimensions obtains the

form

$$\tilde{\mathbf{c}}(\mathbf{x})\cdot\mathbf{u}(\mathbf{x})+\int_S\left\{\bar{\mathbf{P}}^*(\mathbf{x},\mathbf{y})\cdot\mathbf{u}(\mathbf{y})-\bar{\mathbf{U}}^*(\mathbf{x},\mathbf{y})\cdot\mathbf{p}(\mathbf{y})\right\}\mathrm{d}S_y=$$
$$\int_S\left\{\bar{\mathbf{Q}}^*(\mathbf{x},\mathbf{y})\cdot\mathbf{R}(\mathbf{y})-\bar{\mathbf{R}}^*(\mathbf{x},\mathbf{y})\cdot\mathbf{q}(\mathbf{y})\right\}\mathrm{d}S_y+ \tag{50}$$
$$\sum_{C_a}\left\{\bar{\mathbf{U}}^*(\mathbf{x},\mathbf{y})\cdot\mathbf{E}(\mathbf{y})-\bar{\mathbf{E}}^*(\mathbf{x},\mathbf{y})\cdot\mathbf{u}(\mathbf{y})\right\}$$

In case the boundary S is smooth and the point **x** belongs to S, then the integral Eqs (50) and (51) are simplified to

$$\frac{1}{2}\mathbf{u}(\mathbf{x})+\int_S\left\{\bar{\mathbf{P}}^*(\mathbf{x},\mathbf{y})\cdot\mathbf{u}(\mathbf{y})-\bar{\mathbf{U}}^*(\mathbf{x},\mathbf{y})\cdot\mathbf{p}(\mathbf{y})\right\}\mathrm{d}S_y=$$
$$\int_S\left\{\bar{\mathbf{Q}}^*(\mathbf{x},\mathbf{y})\cdot\mathbf{R}(\mathbf{y})-\bar{\mathbf{R}}^*(\mathbf{x},\mathbf{y})\cdot\mathbf{q}(\mathbf{y})\right\}\mathrm{d}S_y \tag{51}$$

Observing Eq. (52), one easily realizes that this equation contains four unknown vector fields, **u(x)**, **p(x)**, **R(x)** and **q(x)** while the boundary conditions are two (classical and non-classical). Thus, the evaluation of the unknown fields requires the existence of one more integral equation. This integral equation is obtained by applying the operator $\partial/\partial n_x$ on (50) and has the form

$$\tilde{\mathbf{c}}(\mathbf{x})\cdot\mathbf{q}(\mathbf{x})+\int_S\left\{\frac{\partial\bar{\mathbf{P}}^*(\mathbf{x},\mathbf{y})}{\partial n_x}\cdot\mathbf{u}(\mathbf{y})-\frac{\partial\bar{\mathbf{U}}^*(\mathbf{x},\mathbf{y})}{\partial n_x}\cdot\mathbf{p}(\mathbf{y})\right\}\mathrm{d}S_y=$$
$$\int_S\left\{\frac{\partial\bar{\mathbf{Q}}^*(\mathbf{x},\mathbf{y})}{\partial n_x}\cdot\mathbf{R}(\mathbf{y})-\frac{\partial\bar{\mathbf{R}}^*(\mathbf{x},\mathbf{y})}{\partial n_x}\cdot\mathbf{q}(\mathbf{y})\right\}\mathrm{d}S_y+ \tag{52}$$
$$\sum_{C_a}\oint_{C_a}\left\{\frac{\partial\bar{\mathbf{U}}^*(\mathbf{x},\mathbf{y})}{\partial n_x}\cdot\mathbf{E}(\mathbf{y})-\frac{\partial\bar{\mathbf{E}}^*(\mathbf{x},\mathbf{y})}{\partial n_x}\cdot\mathbf{u}(\mathbf{y})\right\}\mathrm{d}C_y$$

while for two dimensional and non-smooth boundary is written as

$$\tilde{\mathbf{c}}(\mathbf{x})\cdot\mathbf{q}(\mathbf{x})+\int_S\left\{\frac{\partial\bar{\mathbf{P}}^*(\mathbf{x},\mathbf{y})}{\partial n_x}\cdot\mathbf{u}(\mathbf{y})-\frac{\partial\bar{\mathbf{U}}^*(\mathbf{x},\mathbf{y})}{\partial n_x}\cdot\mathbf{p}(\mathbf{y})\right\}\mathrm{d}S_y=$$
$$\int_S\left\{\frac{\partial\bar{\mathbf{Q}}^*(\mathbf{x},\mathbf{y})}{\partial n_x}\cdot\mathbf{R}(\mathbf{y})-\frac{\partial\bar{\mathbf{R}}^*(\mathbf{x},\mathbf{y})}{\partial n_x}\cdot\mathbf{q}(\mathbf{y})\right\}\mathrm{d}S_y+ \tag{53}$$
$$\sum_{C_a}\left\{\frac{\partial\bar{\mathbf{U}}^*(\mathbf{x},\mathbf{y})}{\partial n_x}\cdot\mathbf{E}(\mathbf{y})-\frac{\partial\bar{\mathbf{E}}^*(\mathbf{x},\mathbf{y})}{\partial n_x}\cdot\mathbf{u}(\mathbf{y})\right\}$$

Finally, for smooth boundaries the above equations obtain the form

$$\begin{aligned}&\frac{1}{2}\mathbf{q}(\mathbf{x})+\int\limits_S\left\{\frac{\partial\bar{\mathbf{P}}^*(\mathbf{x},\mathbf{y})}{\partial n_x}\cdot\mathbf{u}(\mathbf{y})-\frac{\partial\bar{\mathbf{U}}^*(\mathbf{x},\mathbf{y})}{\partial n_x}\cdot\mathbf{p}(\mathbf{y})\right\}\mathrm{d}S_y=\\&\int\limits_S\left\{\frac{\partial\bar{\mathbf{Q}}^*(\mathbf{x},\mathbf{y})}{\partial n_x}\cdot\mathbf{R}(\mathbf{y})-\frac{\partial\bar{\mathbf{R}}^*(\mathbf{x},\mathbf{y})}{\partial n_x}\cdot\mathbf{q}(\mathbf{y})\right\}\mathrm{d}S_y\end{aligned}\tag{54}$$

The pairs of integral equations (50) and (53), (51) and (54), (52) and (55) accompanied by the classical and non-classical boundary conditions form the integral representation of any frequency domain Mindlin's Form II strain gradient elastic boundary value problem with 3D non-smooth boundary, 2D non-smooth boundary and smooth boundary, respectively.

The goal of the boundary element method is to solve numerically the boundary integral representation of the problem presented above. This is done in what follows. For the sake of simplicity only bodies with smooth boundaries are considered. Thus, the smooth boundary S is discretized into e quadratic continuous isoparametric elements each of which has $a(e)$ nodes, with $a(e)$=3, 8, 6 when line, quadrilateral and triangular elements are employed. For a nodal point k, the discretized integral Eqs (52) and (55) for the three dimensional case have the form

$$\begin{aligned}&\frac{1}{2}\mathbf{u}\left(\mathbf{x}^k\right)+\sum_{e=1}^{E}\sum_{a=1}^{A(e)}\int\limits_{-1}^{1}\int\limits_{-1}^{1}\bar{\mathbf{P}}^*\left(\mathbf{x}^k,\mathbf{y}^e\left(\xi_1,\xi_2\right)\right)N^a\left(\xi_1,\xi_2\right)J\left(\xi_1,\xi_2\right)d\xi_1 d\xi_2\cdot\mathbf{u}_a^e\\&+\sum_{e=1}^{E}\sum_{a=1}^{A(e)}\int\limits_{-1}^{1}\int\limits_{-1}^{1}\bar{\mathbf{R}}^*\left(\mathbf{x}^k,\mathbf{y}^e\left(\xi_1,\xi_2\right)\right)N^a\left(\xi_1,\xi_2\right)J\left(\xi_1,\xi_2\right)d\xi_1 d\xi_2\cdot\mathbf{q}_a^e\\&=\sum_{e=1}^{E}\sum_{a=1}^{A(e)}\int\limits_{-1}^{1}\int\limits_{-1}^{1}\bar{\mathbf{U}}^*\left(\mathbf{x}^k,\mathbf{y}^e\left(\xi_1,\xi_2\right)\right)N^a\left(\xi_1,\xi_2\right)J\left(\xi_1,\xi_2\right)d\xi_1 d\xi_2\cdot\mathbf{P}_a^e\\&+\sum_{e=1}^{E}\sum_{a=1}^{A(e)}\int\limits_{-1}^{1}\int\limits_{-1}^{1}\bar{\mathbf{Q}}^*\left(\mathbf{x}^k,\mathbf{y}^e\left(\xi_1,\xi_2\right)\right)N^a\left(\xi_1,\xi_2\right)J\left(\xi_1,\xi_2\right)d\xi_1 d\xi_2\cdot\mathbf{R}_a^e\end{aligned}\tag{55}$$

$$\begin{aligned}
&\frac{1}{2}\mathbf{q}\left(\mathbf{x}^k\right)+\sum_{e=1}^{E}\sum_{a=1}^{A(e)}\int_{-1}^{1}\int_{-1}^{1}\frac{\partial}{\partial n_x}\bar{\mathbf{P}}^*\left(\mathbf{x}^k,\mathbf{y}^e\left(\xi_1,\xi_2\right)\right)N^a\left(\xi_1,\xi_2\right)J\left(\xi_1,\xi_2\right)d\xi_1 d\xi_2\cdot\mathbf{u}_a^e\\
&+\sum_{e=1}^{E}\sum_{a=1}^{A(e)}\int_{-1}^{1}\int_{-1}^{1}\frac{\partial}{\partial n_x}\bar{\mathbf{R}}^*\left(\mathbf{x}^k,\mathbf{y}^e\left(\xi_1,\xi_2\right)\right)N^a\left(\xi_1,\xi_2\right)J\left(\xi_1,\xi_2\right)d\xi_1 d\xi_2\cdot\mathbf{q}_a^e\\
&=\sum_{e=1}^{E}\sum_{a=1}^{A(e)}\int_{-1}^{1}\int_{-1}^{1}\frac{\partial}{\partial n_x}\bar{\mathbf{U}}^*\left(\mathbf{x}^k,\mathbf{y}^e\left(\xi_1,\xi_2\right)\right)N^a\left(\xi_1,\xi_2\right)J\left(\xi_1,\xi_2\right)d\xi_1 d\xi_2\cdot\mathbf{P}_a^e\\
&+\sum_{e=1}^{E}\sum_{a=1}^{A(e)}\int_{-1}^{1}\int_{-1}^{1}\frac{\partial}{\partial n_x}\bar{\mathbf{Q}}^*\left(\mathbf{x}^k,\mathbf{y}^e\left(\xi_1,\xi_2\right)\right)N^a\left(\xi_1,\xi_2\right)J\left(\xi_1,\xi_2\right)d\xi_1 d\xi_2\cdot\mathbf{R}_a^e
\end{aligned}\tag{56}$$

with N_a representing shape functions in local co-ordinate system ξ_1,ξ_2, the first summation is over the elements, the second summation over the element nodes and J is the Jacobian of the transformation from the global coordinate system to the local coordinate system of the element. Finally, u_a^e, q_a^e, p_a^e and R_a^e are the values of the unknown fields at the nodes of element e.

For the two dimensional case, the corresponding discretized equations are:

$$\begin{aligned}
&\frac{1}{2}\mathbf{u}\left(\mathbf{x}^k\right)+\sum_{e=1}^{E}\sum_{a=1}^{A(e)}\int_{-1}^{1}\bar{\mathbf{P}}^*\left(\mathbf{x}^k,\mathbf{y}^e\left(\xi\right)\right)N^a\left(\xi\right)J\left(\xi\right)d\xi\cdot\mathbf{u}_a^e\\
&+\sum_{e=1}^{E}\sum_{a=1}^{A(e)}\int_{-1}^{1}\bar{\mathbf{R}}^*\left(\mathbf{x}^k,\mathbf{y}^e\left(\xi\right)\right)N^a\left(\xi\right)J\left(\xi\right)d\xi\cdot\mathbf{q}_a^e\\
&=\sum_{e=1}^{E}\sum_{a=1}^{A(e)}\int_{-1}^{1}\bar{\mathbf{U}}^*\left(\mathbf{x}^k,\mathbf{y}^e\left(\xi\right)\right)N^a\left(\xi\right)J\left(\xi\right)d\xi\cdot\mathbf{P}_a^e\\
&+\sum_{e=1}^{E}\sum_{a=1}^{A(e)}\int_{-1}^{1}\bar{\mathbf{Q}}^*\left(\mathbf{x}^k,\mathbf{y}^e\left(\xi\right)\right)N^a\left(\xi\right)J\left(\xi\right)d\xi\cdot\mathbf{R}_a^e
\end{aligned}\tag{57}$$

$$\begin{aligned}
&\frac{1}{2}\mathbf{u}\left(\mathbf{x}^k\right)+\sum_{e=1}^{E}\sum_{a=1}^{A(e)}\int_{-1}^{1}\frac{\partial}{\partial n_x}\bar{\mathbf{P}}^*\left(\mathbf{x}^k,\mathbf{y}^e(\xi)\right)N^a(\xi)J(\xi)\,d\xi\cdot\mathbf{u}_a^e\\
&+\sum_{e=1}^{E}\sum_{a=1}^{A(e)}\int_{-1}^{1}\frac{\partial}{\partial n_x}\bar{\mathbf{R}}^*\left(\mathbf{x}^k,\mathbf{y}^e(\xi)\right)N^a(\xi)J(\xi)\,d\xi\cdot\mathbf{q}_a^e\\
&=\sum_{e=1}^{E}\sum_{a=1}^{A(e)}\int_{-1}^{1}\frac{\partial}{\partial n_x}\bar{\mathbf{U}}^*\left(\mathbf{x}^k,\mathbf{y}^e(\xi)\right)N^a(\xi)J(\xi)\,d\xi\cdot\mathbf{P}_a^e\\
&+\sum_{e=1}^{E}\sum_{a=1}^{A(e)}\int_{-1}^{1}\frac{\partial}{\partial n_x}\bar{\mathbf{Q}}^*\left(\mathbf{x}^k,\mathbf{y}^e(\xi)\right)N^a(\xi)J(\xi)\,d\xi\cdot\mathbf{R}_a^e
\end{aligned}\tag{58}$$

with the same notation used for equations (56) and (57).

Next, a global numbering scheme is adopted by assigning a number β to each point (e,a). Then the above equations become

$$\frac{1}{2}\mathbf{u}^k+\sum_{\beta=1}^{L}\tilde{\mathbf{H}}_\beta^k\cdot\mathbf{u}^\beta+\sum_{\beta=1}^{L}\tilde{\mathbf{K}}_\beta^k\cdot\mathbf{q}^\beta=\sum_{\beta=1}^{L}\tilde{\mathbf{G}}_\beta^k\cdot\mathbf{P}^\beta+\sum_{\beta=1}^{L}\tilde{\mathbf{L}}_\beta^k\cdot\mathbf{R}^\beta\tag{59}$$

$$\frac{1}{2}\mathbf{q}^k+\sum_{\beta=1}^{L}\tilde{\mathbf{S}}_\beta^k\cdot\mathbf{u}^\beta+\sum_{\beta=1}^{L}\tilde{\mathbf{T}}_\beta^k\cdot\mathbf{q}^\beta=\sum_{\beta=1}^{L}\tilde{\mathbf{V}}_\beta^k\cdot\mathbf{P}^\beta+\sum_{\beta=1}^{L}\tilde{\mathbf{W}}_\beta^k\cdot\mathbf{R}^\beta\tag{60}$$

where L is the total number of nodes. Note that Eqs (60) and (61) are valid for both the 2D and the 3D case. However, the integrals $\tilde{\mathbf{H}}$, $\tilde{\mathbf{K}}$, $\tilde{\mathbf{G}}$, $\tilde{\mathbf{L}}$, $\tilde{\mathbf{S}}$, $\tilde{\mathbf{T}}$, $\tilde{\mathbf{V}}$, $\tilde{\mathbf{W}}$ are different in each case.

Namely, for the 3D case

$$\tilde{\mathbf{H}}_\beta^k=\int_{-1}^{1}\int_{-1}^{1}\tilde{\mathbf{P}}^*\left(\mathbf{x}^k,\mathbf{y}^e(\xi_1,\xi_2)\right)N^a(\xi_1,\xi_2)J(\xi_1,\xi_2)\,d\xi_1 d\xi_2\Big|_{(e,a)\to\beta}$$

$$\tilde{\mathbf{K}}_\beta^k=\int_{-1}^{1}\int_{-1}^{1}\tilde{\mathbf{R}}^*\left(\mathbf{x}^k,\mathbf{y}^e(\xi_1,\xi_2)\right)N^a(\xi_1,\xi_2)J(\xi_1,\xi_2)\,d\xi_1 d\xi_2\Big|_{(e,a)\to\beta}$$

$$\tilde{\mathbf{G}}_\beta^k=\int_{-1}^{1}\int_{-1}^{1}\tilde{\mathbf{U}}^*\left(\mathbf{x}^k,\mathbf{y}^e(\xi_1,\xi_2)\right)N^a(\xi_1,\xi_2)J(\xi_1,\xi_2)\,d\xi_1 d\xi_2\Big|_{(e,a)\to\beta}$$

$$\begin{aligned}
\tilde{\mathbf{L}}_{\beta}^{k} &= \int_{-1}^{1}\int_{-1}^{1} \tilde{\mathbf{Q}}^{*}\left(\mathbf{x}^{k},\mathbf{y}^{e}\left(\xi_1,\xi_2\right)\right) N^{a}\left(\xi_1,\xi_2\right) J\left(\xi_1,\xi_2\right) d\xi_1 d\xi_2 \Big|_{(e,a)\to\beta} \\
\tilde{\mathbf{S}}_{\beta}^{k} &= \int_{-1}^{1}\int_{-1}^{1} \frac{\partial}{\partial n_x}\tilde{\mathbf{P}}^{*}\left(\mathbf{x}^{k},\mathbf{y}^{e}\left(\xi_1,\xi_2\right)\right) N^{a}\left(\xi_1,\xi_2\right) J\left(\xi_1,\xi_2\right) d\xi_1 d\xi_2 \Big|_{(e,a)\to\beta}
\end{aligned} \tag{61}$$

$$\begin{aligned}
\tilde{\mathbf{T}}_{\beta}^{k} &= \int_{-1}^{1}\int_{-1}^{1} \frac{\partial}{\partial n_x}\tilde{\mathbf{R}}^{*}\left(\mathbf{x}^{k},\mathbf{y}^{e}\left(\xi_1,\xi_2\right)\right) N^{a}\left(\xi_1,\xi_2\right) J\left(\xi_1,\xi_2\right) d\xi_1 d\xi_2 \Big|_{(e,a)\to\beta} \\
\tilde{\mathbf{V}}_{\beta}^{k} &= \int_{-1}^{1}\int_{-1}^{1} \frac{\partial}{\partial n_x}\tilde{\mathbf{U}}^{*}\left(\mathbf{x}^{k},\mathbf{y}^{e}\left(\xi_1,\xi_2\right)\right) N^{a}\left(\xi_1,\xi_2\right) J\left(\xi_1,\xi_2\right) d\xi_1 d\xi_2 \Big|_{(e,a)\to\beta} \\
\tilde{\mathbf{W}}_{\beta}^{k} &= \int_{-1}^{1}\int_{-1}^{1} \frac{\partial}{\partial n_x}\tilde{\mathbf{Q}}^{*}\left(\mathbf{x}^{k},\mathbf{y}^{e}\left(\xi_1,\xi_2\right)\right) N^{a}\left(\xi_1,\xi_2\right) J\left(\xi_1,\xi_2\right) d\xi_1 d\xi_2 \Big|_{(e,a)\to\beta}
\end{aligned}$$

and for the 2D case

$$\begin{aligned}
\tilde{\mathbf{H}}_{\beta}^{k} &= \int_{-1}^{1} \tilde{\mathbf{P}}^{*}\left(\mathbf{x}^{k},\mathbf{y}^{e}\left(\xi\right)\right) N^{a}\left(\xi\right) J\left(\xi\right) d\xi \Big|_{(e,a)\to\beta} \\
\tilde{\mathbf{K}}_{\beta}^{k} &= \int_{-1}^{1} \tilde{\mathbf{R}}^{*}\left(\mathbf{x}^{k},\mathbf{y}^{e}\left(\xi\right)\right) N^{a}\left(\xi\right) J\left(\xi\right) d\xi \Big|_{(e,a)\to\beta} \\
\tilde{\mathbf{G}}_{\beta}^{k} &= \int_{-1}^{1} \tilde{\mathbf{U}}^{*}\left(\mathbf{x}^{k},\mathbf{y}^{e}\left(\xi\right)\right) N^{a}\left(\xi\right) J\left(\xi\right) d\xi \Big|_{(e,a)\to\beta}
\end{aligned}$$

$$\begin{aligned}
\tilde{\mathbf{L}}_{\beta}^{k} &= \int_{-1}^{1} \tilde{\mathbf{Q}}^{*}\left(\mathbf{x}^{k},\mathbf{y}^{e}\left(\xi\right)\right) N^{a}\left(\xi\right) J\left(\xi\right) d\xi \Big|_{(e,a)\to\beta} \\
\tilde{\mathbf{S}}_{\beta}^{k} &= \int_{-1}^{1} \frac{\partial}{\partial n_x}\tilde{\mathbf{P}}^{*}\left(\mathbf{x}^{k},\mathbf{y}^{e}\left(\xi\right)\right) N^{a}\left(\xi\right) J\left(\xi\right) d\xi \Big|_{(e,a)\to\beta}
\end{aligned} \tag{62}$$

$$\tilde{\mathbf{T}}_{\beta}^{k} = \int_{-1}^{1} \frac{\partial}{\partial n_x} \tilde{\mathbf{R}}^{*}\left(\mathbf{x}^{k}, \mathbf{y}^{e}(\xi)\right) N^{a}(\xi) J(\xi) d\xi \Bigg|_{(e,a)\to\beta}$$

$$\tilde{\mathbf{V}}_{\beta}^{k} = \int_{-1}^{1} \frac{\partial}{\partial n_x} \tilde{\mathbf{U}}^{*}\left(\mathbf{x}^{k}, \mathbf{y}^{e}(\xi)\right) N^{a}(\xi) J(\xi) d\xi \Bigg|_{(e,a)\to\beta}$$

$$\tilde{\mathbf{W}}_{\beta}^{k} = \int_{-1}^{1} \frac{\partial}{\partial n_x} \tilde{\mathbf{Q}}^{*}\left(\mathbf{x}^{k}, \mathbf{y}^{e}(\xi)\right) N^{a}(\xi) J(\xi) d\xi \Bigg|_{(e,a)\to\beta}$$

When $\beta \neq k$ the above integrals are non-singular and can be easily computed through Gauss quadrature. In the case of $\beta = k$ the integrals become singular and special treatment is required. This is accomplished by applying the methodology proposed by Guiggiani (1998) for singular integrations. Perhaps it would be more convenient here to use a regularization technique for converting all hypersingular integrals appearing in the integral equations (51)-(55) into weakly singular ones before any numerical solution (Okada, Rajiyah and Atluri (1988,1990), Han and Atluri (2002), Han, Yao and Atluri (2005), Liu (2007,2009)). Actually, this could be the subject if a future paper.

Systems (60) and (61) form the following linear system of algebraic equations

$$\begin{bmatrix} \frac{1}{2}\tilde{\mathbf{I}}+\mathbf{H} & \mathbf{K} \\ \mathbf{S} & \frac{1}{2}\tilde{\mathbf{I}}+\mathbf{T} \end{bmatrix} \cdot \begin{Bmatrix} \mathbf{u} \\ \mathbf{q} \end{Bmatrix} = \begin{bmatrix} \mathbf{G} & \mathbf{L} \\ \mathbf{V} & \mathbf{W} \end{bmatrix} \cdot \begin{Bmatrix} \mathbf{p} \\ \mathbf{R} \end{Bmatrix} \tag{63}$$

which after the application of the classical and non-classical boundary conditions and rearranging, the following final linear system is obtained

$$[\mathbf{A}] \cdot \{\mathbf{X}\} = \{\mathbf{B}\} \tag{64}$$

where the vectors $\mathbf{X}$ and $\mathbf{B}$ contain all the unknown and known nodal components of the boundary fields respectively.

Finally, the linear system (65) is solved via a typical LU-decomposition algorithm and the vector $\mathbf{X}$, comprising all the unknown nodal values of $\mathbf{u}$, $\mathbf{q}$, $\mathbf{R}$ and $\mathbf{P}$, is evaluated.

5 Numerical Examples

In this section 2D and 3D harmonic numerical examples that demonstrate the accuracy of the proposed BEM are presented.

The first benchmark deals with an infinitely extended hollow cylinder clumped internally and subjected to an external radial harmonic displacement u_0 with frequency ω. Considering plane strain conditions with radial symmetry, this problem under the classical boundary conditions $u(a)=0,\ u(b)=u_0$ and the non-classical ones $q(a)=q(b)=0$ admits an analytical solution of the form

$$\begin{aligned} u(r) &= A_c J_1(\zeta_1 r) + B_c H_1^{(1)}(\zeta_1 r) + C_c J_1(\zeta_2 r) + D_c H_1^{(1)}(\zeta_2 r) \\ \zeta_{1,2} &= \sqrt{\frac{k_p^2 h_1^2 - 1 \pm \sqrt{\left(k_p^2 h_1^2 - 1\right)^2 + 4k_p^2 \ell_1^2}}{2\ell_1^2}} \\ k_p^2 &= \frac{\rho\omega^2}{\lambda + 2\mu} \end{aligned} \tag{65}$$

where a,b represent the inner and outer radii of the cylinder and $J_1(\bullet)$ are Bessel functions of first kind and first order and $H_1^{(1)}(\bullet)$ are Hankel functions of fist kind and first order.

Also, the case with the non-classical boundary conditions $R(a)=R(b)=0$ has been considered. The constants a_c, B_c, C_c, D_c are easily calculated via the algebraic system the four boundary conditions form. As it is expected, due to the radial symmetry of the problem only the longitudinal intrinsic parameters ℓ_1^2, h_1^2 are involved in the expression of the analytical solution (67).

In the sequel, the same plain strain problem is numerically solved with the BEM demonstrated in the previous section. Due to the symmetry only the one quadrant of the cross-section is considered. The material constants assumed are $E = 1.4\ GPa, \nu = 0.37, \rho = 1500\ kg/m^3$while the internal and external radii of the cylinder are taken equal to $a = 1\ cm, b = 8\ cm$.

Figure 1 depicts the calculated radial displacements and radial strains through thickness for the frequency of $\omega = 10^5 rad/\sec$ and for different combinations of the intrinsic parametersℓ_1^2, h_1^2. Numerical results corresponding to double tractions non-classical boundary conditions are indicated in Figure 1 by the letter "R". The numerical results are compared to the corresponding analytical ones and as it is apparent the agreement is excellent.

The second numerical example concerns a spherical cavity of radius $a = 5\ cm$ embedded into the gradient elastic medium of the previous benchmark and subjected to an internal uniform harmonic displacement $u_0 = 1\ mm$.Considering the classical boundary condition $u(a) = u_0$ and the non-classical one $q(a) = 0$; it is easy to find

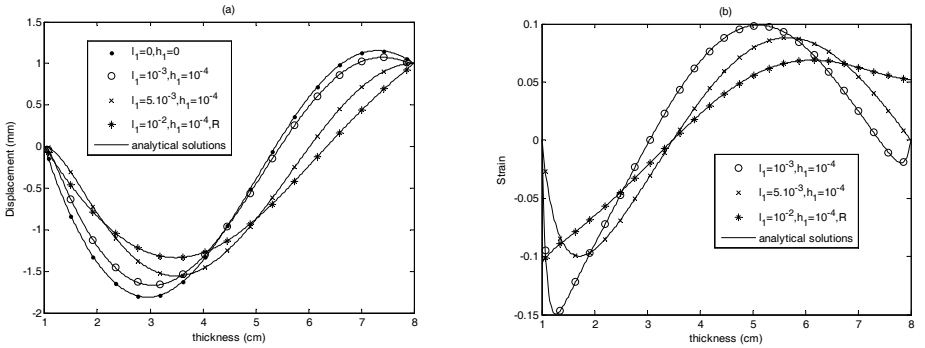

Figure 1: Radial displacements (a) and strains (b) through thickness for an infinitely extended gradient elastic hollow cylinder clamped internally and subjected externally to a harmonic radial displacement $u_0 = 1\ mm$ of frequency $\omega = 10^5 rad/\sec$.

one that its analytical solution is of the form

$$\begin{aligned} u(r) &= A_c h_1^{(1)}(\zeta_1 r) + B_c h_1^{(1)}(\zeta_2 r) \\ \zeta_{1,2}^2 &= \sqrt{\frac{k_p^2 h_1^2 - 1 \pm \sqrt{\left(k_p^2 h_1^2 - 1\right)^2 + 4k_p^2 \ell_1^2}}{2\ell_1^2}} \\ k_p^2 &= \frac{\rho\omega^2}{\lambda + 2\mu} \end{aligned} \tag{66}$$

where $h_1^{(1)}(\bullet)$ represents spherical Hankel functions of first order and first kind. The constants A_c, B_c are easily calculated via the algebraic system the two boundary conditions form.

The corresponding BEM solution is accomplished by discretizing one octant of the sphere with quadratic quadrilateral elements. A set of internal points have been considered, so that both radial displacement and radial strains are evaluated.

Figure 2 depicts the calculated radial displacements and radial strains on the considered internal points for the frequency of $\omega = 10^5 rad/\sec$ and for different combinations of the intrinsic parameters ℓ_1^2, h_1^2. The numerical results are compared to the corresponding analytical ones of Eq. (67) and as it is apparent the agreement is excellent.

The third example is illustrated in Figure 3. Consider a gradient elastic half-space with material constants $E = 14\ GPa, \nu = 0.37, \rho = 1500\ kg/m^3$ and two different internal length scale parameters provided in Table 1.

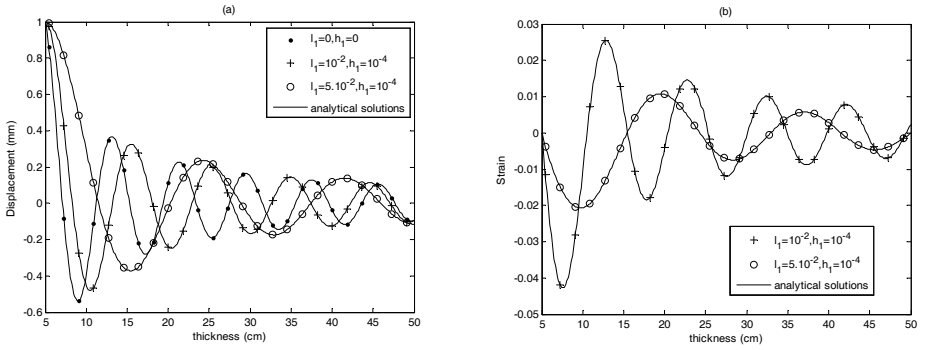

Figure 2: Radial displacements (a) and strains (b) for a spherical cavity embedded in a gradient elastic material and subjected to a harmonic radial displacement $u_0 = 1\ mm$ of frequency $\omega = 10^5 rad/\sec$

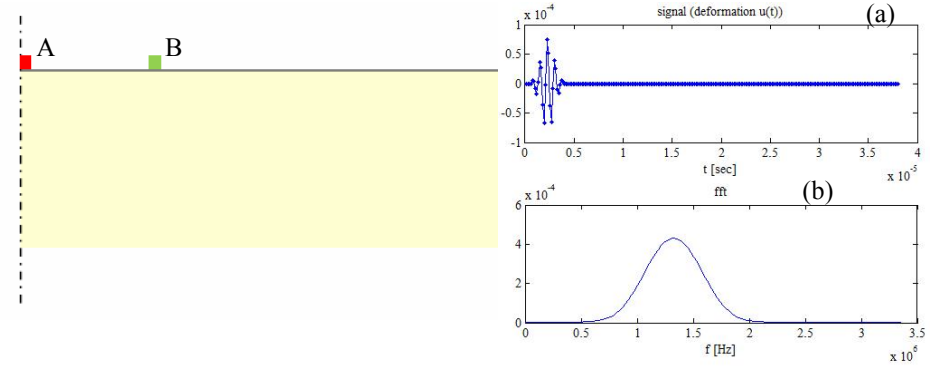

Figure 3: Gradient elastic half space subjected to an impulsive traction excitation at A with time history (a) and FFT frequency spectrum (b).

An impulsive traction excitation is imposed at point A and the generalized Rayleigh wave propagates across the free surface of the half-space. For the sake of simplicity symmetry at point A has been considered. Discretizing the free surface of the half-space and taking the BEM solutions for each frequency of the Fast Fourier Transform (FFT) spectrum shown in Figure 3(b), the time history of point B is calculated. Four quadratic line elements per wavelength corresponding to central frequency have been used for the discretization of the free space. The transient solution is obtained after inversion of frequency domain results via the inverse FFT.

Table 1: Intrinsic gradient elastic parameters for the problem depicted in Fig. 3

	Case 1	Case 2
$\hat{a}_1$	0.0	0.0
$\hat{a}_2$	72.71	78.645
$\hat{a}_3$	0.0	0.0
$\hat{a}_4$	51.095	55.264
$\hat{a}_5$	0.0	0.0
ℓ_1^2	10^{-8}	$(1.04)^2 10^{-8}$
ℓ_2^2	10^{-8}	$(1.04)^2 10^{-8}$
h_1^2	10^{-10}	$(1.04)^2 10^{-8}$
h_2^2	10^{-10}	$(0.74)^2 10^{-8}$

The signal at point B is converted to time-frequency domain through the Reassigned Smoothed Pseudo Wigner- Ville transform illustrated in Vavourakis, Protopappas, Fotiadis and Polyzos (2009). The results are shown in Figures 4 and 5 in the form of pseudo-color images, where the color of a point represents the amplitude (in dB) of the energy distribution. In both figures the time-frequency representation of the first symmetric (solid line) and antisymmetric (dash line) mode corresponding to the propagation of a pulse in a free of traction gradient elastic plate, obtained analytically by Vavva, Protopappas, Gergidis, Charalambopoulos, Fotiadis and Polyzos (2009) for the case 1 of Table 1, are also depicted.

Observing Figs 4 and 5 one can say that (i) BEM solutions justify the dispersion nature of Rayleigh waves in gradient elastic media (Georgiadis, Vardoulakis and Lykotrafitis (2000), Georgiadis and Velgaki (2003)) (ii) the dispersion line of the Rayleigh wave is obtained asymptotically by the plate first symmetric and antisymmetric mode as in the case of the classical elasticity and (iii) the dispersion only depends on the values of the internal stiffness and inertia microstructural parameters.

6 Conclusions

A boundary element method for solving two and three-dimensional dynamic strain gradient elastic problems in the context of Mindlin's Form II strain gradient elastic theory has been developed. The equation of motion, all the possible boundary conditions (classical and non-classical), the fundamental solution and the reciprocity identity of the gradient elastic problem are explicitly presented. Both, fundamental solution and reciprocity identity have been used to establish the boundary integral representation of the problem consisting of one equation for the displacement

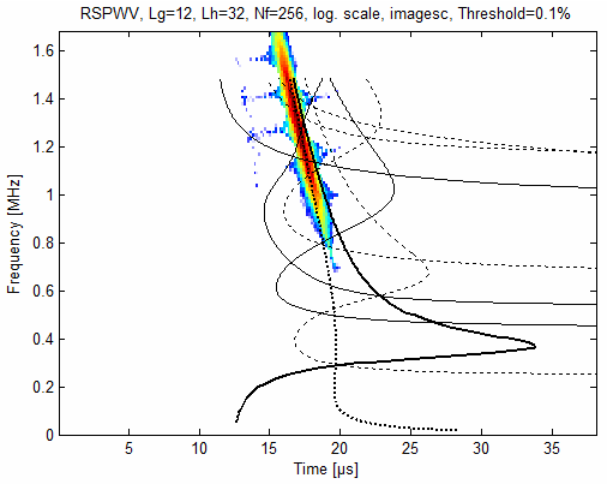

Figure 4: Time–frequency representation of vertical displacement at point B of Figure 3 for the case 1 of Table 1. Solid and dash lines represent symmetric and antisymmetric modes, respectively, corresponding to the propagation of a pulse in a free of traction gradient elastic plate, obtained analytically by Vavva, Protopappas, Gergidis, Charalambopoulos, Fotiadis and Polyzos (2009).

and another one for its normal derivative. The numerical implementation of the problem is accomplished by discretizing the external boundary into quadratic line or quadrilateral/triangular elements, while the numerical evaluation of all integrals with any order of singularity is accomplished directly with the aid of advanced integration algorithms. Three representative numerical examples have been presented to illustrate the method, demonstrate its high accuracy and confirm the effect of the microstructure to macrostructure.

References

Askes, H.; Bennett, T.; Aifantis, E. C. (2007): A new formulation and C0-implementation of dynamically consistent gradient elasticity, *Int. J. Numer. Meth. Engng*; 72:111–126.

Askes, H.; Wang, B.; Bennett, T. (2008): Element size and time step selection procedures for the numerical analysis of elasticity with higher-order inertia, *Journal of Sound and Vibration* 314 650–656.

Atluri, S.N. (2004): *The meshless method (MLPG) for domain & BIE discretizations*, Tech Science Press, USA.

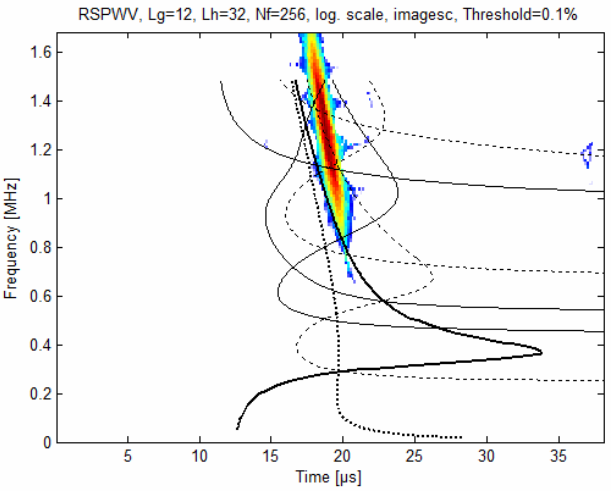

Figure 5: Time–frequency representation of vertical displacement at point B of Figure 3 for the case 2 of Table 1. Solid and dash lines represent symmetric and antisymmetric mode, respectively, corresponding to the propagation of a pulse in a free of traction gradient elastic plate, obtained analytically by Vavva, Protopappas, Gergidis, Charalambopoulos, Fotiadis and Polyzos (2009) for the case 1 of Table 1.

Atluri, S.N; Shen, S. (2002): The meshless Local Petrov-Galerkin (MLPG) Method: a simple & less-costly alternative to the Finite Element and Boundary Element Methods, *CMES: Computer Modeling in Engineering & Sciences*, 3(1), 11-51.

Atluri, S. N.; Zhu, T. (1998): A new meshless local Petrov-Galerkin (MLPG) approach in computation mechanics. *Computational Mechanics*, vol. 22, pp. 117–127.

Bennett, T.; Askes, H. (2009): Finite element modelling of wave dispersion with dynamically consistent gradient elasticity, *Comput Mech* 43:815–825.

Beskos D. E. (1987): Boundary element methods in dynamic analysis, *Appl. Mech. Rev. ASME*, 40, 1–23.

Beskos D. E (1997): Boundary element methods in dynamic analysis. part II (1986–1996). *Appl. Mech. Rev. ASME*, 50, 149–197.

Chen, Y.; Lee, J.D.; Eskandarian, A. (2004): Micropolar theory and its applications to mesoscopic and microscopic problems, *CMES: Computer Modeling in Engineering & Sciences*, 5(1), 35-44.

Cosserat, E.; Cosserat, F. (1909): *Theorie des Corps Deformables*, Cornell Uni-

versity Library.

Eringen, **A. C.** (1999): *Microcontinuum Field Theories I: Foundations and Solids*. Springer-Verlang, New York.

Eringen, **A. C.** (1992): Vistas of nonlocal continuum physics, *Int. J. Engng Sci.*, 30, 1551–1565.

Exadaktylos, G. E.; Vardoulakis I. (2001): Microstructure in linear elasticity and scale effects: a reconsideration of basic rock mechanics and rock fracture mechanics. *Tectonophysics*, 335, 81–109.

Georgiadis, HG (2003) The mode III crack problem in microstructured solids governed by dipolar gradient elasticity: Static and dynamic analysis. *Journal of Applied Mechanics-Transactions of the ASME* 70 (4): 517-530.

Georgiadis, HG; Vardoulakis, I; Lykotrafitis, G (2000) Torsional surface waves in a gradient-elastic half-space. *Wave Motion* 31: 333-348.

Georgiadis, HG; Velgaki, EG (2003) High frequency Reyleigh waves in materials with microstructure and couple stress effects. *Int. J. Solids Structures* 40: 2501-2520.

Giannakopoulos, A. E.; Amanatidou, E.; Aravas, N. (2006): A reciprocity theorem in linear gradient elasticity and the corresponding Saint-Venant principle. *Int. J. Solids Struct.*, 43, 3875–3894.

Green, A. E. ; Rivlin, R. S. (1964): Multipolar continuum mechanics, *Arch. Ration. Mech. Anal.*, 17, 113–147.

Guiggiani, M. (1998): Formulation and numerical treatment of the boundary integral equations with hypersingular kernels, 448. *Computational Mechanics*, Inc., Southampton.

Han, Z.D.; Atluri, S.N. (2002): SGBEM (for Cracked Local Subdomain) – FEM (for uncracked global Structure) alternating method for analyzing 3D surface cracks and their fatigue-growth, *CMES: Computer Modeling in Engineering & Sciences*, 3(6), 699-716.

Han, Z.D.; Atluri, S.N. (2004): Meshless Local Petrov-Galerkin (MLPG) approaches for solving 3D problems in elasto-statics, *CMES: Computer Modeling in Engineering & Sciences*, 6(2), 169-188.

Han, Z; Yao, Z.; Atluri, S.N. (2005): Weakly-singular traction and displacement boundary integral equations and their Meshless Local Petrov-Galerkin approaches, *Tsinghua Science & Technology*, 10(1), 1-7.

Huang, F-Y.; Liang K-Z. (1997): Boundary element analysis of stress concentration in micropolar elastic plate, *Int. J. Num. Methods Engng.* 40, 1611-1622.

Kadowaki, H; Liu, W.K. (2005): A multiscale approach for the micropolar continuum model, *CMES: Computer Modeling in Engineering & Sciences*, 7(3), 269-282.

Karlis, Charalambopoulos and Polyzos (2010 – In Press): An advanced boundary element method for solving 2D and 3D static problems in Mindlin's strain-gradient theory of elasticity, *International Journal for Numerical Methods in Engineering*, DOI: 10.1002/nme.2862.

Karlis, G. F. ; Tsinopoulos, S. V. ; Polyzos, D.; Beskos, D. E. (2008): 2D and 3D boundary element analysis of mode-i cracks in gradient elasticity, *CMES: Computer Modeling in Engineering & Sciences*, 26, 189–207.

Karlis, G. F. ; Tsinopoulos, S. V. ; Polyzos, D.; Beskos, D. E. (2007): Boundary element analysis of mode i and mixed mode (i and ii) crack problems of 2-d gradient elasticity, *Comput. Methods Appl. Mech. Engrg.*, 196, 5092–5103.

Koiter, W.T.(1964): Couple stress in the theory of elasticity I-II, *Proc. Kon. Nederl. Akad. Wetensch.*, B 67, 17–44.

Liang, K-Z.; Liang F-Y. (1996): Boundary element method for micropolar elasticity, *Int. J. Engng Sci*. 35(5), 509-521.

Liu, C-S. (2007): A MRIEM for solving the Laplace equation in the doubly-connected domain, *CMES: Computer Modeling in Engineering & Sciences*, 19(2), 145,162.

Liu, C-S. (2009): A new method for Fredholm integral equations of 1D backward heat conduction problems, *CMES: Computer Modeling in Engineering & Sciences*, 47(1), 1-22.

Markolefas, S. I.; Tsouvalas, ,D.A.; Tsamasphyros, G. I. (2009): Mixed finite element formulation for the general anti-plane shear problem, including mode III crack computations, in the framework of dipolar linear gradient elasticity, *Comp. Mech.*, 43, 715–730.

Markolefas, S. I.; Tsouvalas, D. A. ; Tsamasphyros, G. I. (2007): Theoretical analysis of a class of mixed, C0 continuity formulations for general dipolar gradient elasticity boundary value problems. *Int. J. Solids Struct.*, 44, 546–572.

Mindlin, R. D. (1964): Micro-structure in linear elasticity, *Arch. Rat. Mech. Anal.*, 16, 51–78.

Mindlin, R. D. (1965): Second gradient of strain and surface-tension in linear elasticity, *International Journal of Solids and Structures*, 1, 417–438.

Mindlin, R. D.; Tiersten, H. F. (1962): Effects of couple stresses in linear elasticity, *Arch. Rat. Mech. Anal.*, 11, 415–448.

Okada, H; Rajiyah, H.; Atluri, S.N. (1988): Some recent development in finite-strain elastoplasticity using the field-boundary element method, *Computers & Struc-*

tures, 30(1/2), 275-288.

Okada, H; Rajiyah, H.; Atluri, S.N. (1990): A full tangent stiffness field-boundary element formulation for geometric and material nonlinear problems of solid mechanics, *Int. J. for Numerical Methods in Engineering*, 29, 15-35.

Papanicolopulos, S. A.; Zervos, A.; Vardoulakis, I. (2009): A three dimensional C(1) finite element for gradient elasticity, *Int. J. Numer. Meth. Engng.*, 77, 1396–1415.

Polyzos, D. (2005): 3D frequency domain bem for solving dipolar gradient elastic problems, *Comput Mech*, 35, 292–304.

Polyzos, D.; Tsepoura, K. G.; Beskos, D. E. (2005): Transient dynamic analysis of 3-d gradient elastic solids by BEM, *Comput. Struct.*, 83, 783–792.

Polyzos, D.; Tsepoura, K. G.; Tsinopoulos, S. V.; Beskos, D. E. (2003): A boundary element method for solving 2-d and 3-d static gradient elastic problems. part I: Integral formulation, *Comput. Meth. Appl. Mech. Engng*, 192, 2845–2873.

Sladek, J; Sladek, V. (2003): Application of local boundary integral equation method into micropolar elasticity, *Eng. Anal with Boundary Elements*, 27, 81-90.

Sladek, J.; Sladek, V. (1985): Boundary element method in micropolar thermoelasticity Part III: Numerical Solution, *Engn Analysis 2*, 155-162.

Sladek, J.; Sladek, V.; Solek, P. (2009): Elastic analyses in 3D anisotropic functionally graded solids by the MLPG, *CMES: Computer Modeling in Engineering & Sciences*, 43, 223-251.

Sladek, V.; Sladek, J. (1985): Boundary element method in micropolar thermoelasticity Part I: Boundary Integral Equations, *Engn Analysis 2*, 40-50.

Sladek, V.; Sladek, J. (1985): Boundary element method in micropolar thermoelasticity Part II: Boundary Integro-differential Equations, *Engn Analysis 2*, 81-91.

Tang, A.; Shen, S.; and Atluri, S.N. (2003): Analysis of Materials with Strain-Gradient Effects: A Meshless Local Petrov-Galerkin(MLPG) Approach, with Nodal Displacements only, *CMES: Computer Modeling in Engineering & Sciences*, vol.4, no.1, pp.177-196.

Teneketzis, L.; Aifantis, E.C. (2002): A two-dimensional Finite Element Implementation of a special form of gradient elasticity, *CMES: Computer Modeling in Engineering & Sciences*, 3(6), 731-742.

Toupin R. A. (1964): Theories of elasticity with couple-stress, *Arch. Rat. Mech. Anal.*, 17, 85–112.

Tsepoura, K.G.; Papargyri-Beskou, S.; Polyzos, D. (2002): A boundary element method for solving 3D static gradient elastic problems with surface energy. *Com-*

put. Mech. 29, pp. 361-381.

Tsepoura, K. G.; Polyzos, D. (2003): Static and harmonic bem solutions of gradient elasticity problems with axisymmetry, *Comput. Mech.*, 32, pp. 89–103.

Tsepoura, K.G.; Tsinopoulos, S.V.; Polyzos, D.; Beskos, D.E. (2003): A boundary element method for solving 2-d and 3-d static gradient elastic problems. part ii: Numerical implementation, *Comput. Meth. Appl. Mech. Engng*., 192, pp. 2875–2907.

Vardoulakis, I.; Sulem, J. (1995): *Bifurcation Analysis in Geomechanics*. Blackie Chapman and Hall, London.

Vavourakis, V.; Protopappas, V. I. C.; Fotiadis, D.; Polyzos, D. (2009): Numerical determination of modal dispersion and AE signal characterization in waveguides through LBIE/BEM and time–frequency analysis, *Comput Mech.* 43. pp. 431–441.

Vavva, M.G.; Protopappas, V.C.; Gergidis L.N.; Charalambopoulos, A.; Fotiadis, D.I.; Polyzos, D. (2009): Velocity dispersion of guided waves propagating in a free gradient elastic plate: Application to cortical bone, *J. Acoust. Soc. Am.*, 125 _5, May, pp. 3414-3427.

Xie, G.Q.; Long, S.Y. (2006): Elastic vibration behaviors of carbon nanotubes based on micropolar mechanics, *CMC: Computers, Materials & Continua*, 4(1) 11-20.

Zervos, A. (2008): Finite elements for elasticity with microstructure and gradient elasticity, *Int. J. Numer. Meth. Engng*, 73, pp. 564–595.

Zervos, A.; Papanicolopulos, S. A.; Vardoulakis, I. (2009): Two finite element discretizations for gradient elasticity, *J. Engrg. Mech. (ASCE)*, 135, pp. 203–213.

Zhu, T.; Zhang, J. D.; Atluri, S. N. (1998): A local boundary integral equation (LBIE) method in computational mechanics and a meshless discretization approach. *Computational Mechanics*, vol. 21, pp. 223–235.